JOURNAL OF CATALYSIS 124, 301–314 (1990)

Molybdenum-oxo Species Deposited on Alumina by Adsorption

I. Mechanism of the Adsorption

N. SPANOS, L. VORDONIS, CH. KORDULIS, AND A. LYCOURGHIOTIS[1]

Department of Chemistry and the Research Institute of Chemical Engineering and Chemical Processes at High Temperatures, P.O. Box 1239, University Campus, GR-26110 Patras, Greece

Received June 13, 1989; revised February 14, 1990

The mechanism of adsorption of molybdates on the surface of γ-alumina was investigated by use of adsorption equilibrium experiments, potentiometric titrations, microelectrophoresis and UV/VIS spectroscopy. From the experimental results and the theoretical analysis of the isotherms it was concluded that Mo^{VI} deposition was done by adsorption of the $Mo_xO_y^{z-}$ ions on energetically equivalent and distinct sites of the inner Helmholtz plane (IHP) of the double layer on the surface of the γ-alumina particles suspended in the aqueous medium. The creation of these sites was mainly attributed to the presence of the protonated surface hydroxyls of γ-alumina and not to the neutral hydroxyls. Analysis of the adsorption isotherms suggested that considerable lateral interactions are exerted between the adsorbed $Mo_xO_y^{z-}$ ions, resulting in the formation of $Mo_xO_y^{z-}$ . . . $Mo_xO_y^{z-}$ . . . oligomers in the IHP. It is proposed that these polymeric ions are deposited on the surface in the drying step.

INTRODUCTION

Although numerous investigations have been devoted to the preparation and surface chemistry of molybdena-supported γ-alumina catalysts, the mechanism by which the molybdate anions (present in the typical ammonium heptamolybdate solutions usually used, e.g., MoO_4^{2-}, $Mo_7O_{24}^{6-}$) are deposited on the support surface remains unclear. A reason for this is presumably that, for the most part, work done so far has been focused on the characterization of dried or calcined catalysts prepared by methods (dry or wet impregnation followed by drying) favoring the deposition of the supported phase by *both* adsorption and precipitation. Studies dealing with catalysts prepared by equilibrium adsorption followed by filtration are scarce in the literature (*1–5*). An understanding of the mechanism of adsorption requires an answer to the following questions: (i) Which are the main surface groups of γ-alumina responsible for the creation of the sorptive sites: The neutral (*3, 5–8*) or the protonated surface hydroxyls (*1, 2, 4, 9, 10*)? (ii) Are polymolybdates dissociated to MoO_4^{2-} prior to adsorption (*3, 6, 8, 10–13*) or are they adsorbed undissociated (*1, 2, 14, 15*)? (iii) In which part of the double layer, surrounding the γ-alumina particles suspended in the impregnating solution, are the molybdate ions located? On the surface of the carrier, the inner Helmholtz plane (IHP), or in the diffuse part of the double layer? (iv) Are the lateral interactions between the molybdate ions resulting in the formation of polymeric surface molybdate species developed before or after drying? (v) Is the adsorption of molybdate species localized or nonlocalized?

The purpose of the present work is to clarify the mechanism of adsorption of molybdates on the surface of γ-alumina by answering the above-mentioned questions. To answer the first question we compared adsorption data with surface concentrations of neutral and protonated surface hydroxyls regulated by changing the temperature

[1] To whom all correspondence should be addressed.

0021-9517/90 $3.00

or pH (*16*) of the impregnating solution and doping the carrier (*17–19*). The theoretical analysis of the adsorption isotherms, by derivation and testing several equations, allowed us to approach points (ii)–(v). The answer to the third question is corroborated by potentiometric titrations and microelectrophoretic mobility measurements.

The present paper is the first part of a work aimed at the study of molybdena/γ-alumina catalysts prepared by adsorption equilibrium using γ-alumina-based carriers with controlled concentration of charged surface groups.

EXPERIMENTAL

Materials

The support used in the present study was obtained by crushing Houdry Ho 415 γ-alumina extrudates (S_{BET} = 123 m^2/g, water pore volume = 0.45 cm^3/g). After sieving, a fraction between 100–150 mesh was selected, impregnated with bidistilled water, dried at 120°C for 2.5 h and calcined at 600°C for 12 h.

The ammonium heptamolybdate, obtained from Riedel de Haen (99%), was used for the preparation of the molybdate aqueous solutions used in the adsorption experiments as well as in some potentiometric titration and microelectrophoretic mobility measurements. The ammonium nitrate, obtained from Riedel de Haen (99%), was used for the preparation of the aqueous solutions of the background electrolyte employed in some potentiometric titration and microelectrophoretic mobility measurements as well as for regulating the ionic strength of the molybdate solutions used in the adsorption experiments.

Equilibrium Adsorption

Equilibrium adsorption experiments were performed at 25.0 ± 0.1°C and pH 5.0 ± 0.1 (i.e., suspension of γ-Al_2O_3 adjusted the pH to the final value of 5.0 ± 0.1). It should be noted that the amount of acid or base added was low enough to avoid any alteration in the ionic strength of the solution. The regulation of the ionic strength at 0.1 *M* was done using NH_4NO_3 aqueous solutions. It was observed that the molybdate solutions containing NH_4NO_3 were quite stable for long periods of time. In each experiment a volume of 0.015 dm^3 of molybdate solution of various concentrations, ranging between (10^{-3}–3 × 10^{-2}) mol Mo^{VI}/dm^3, was placed in a small polyethylene vial, thermostated in a double-walled, water-jacketed vessel at 25.0 ± 0.1°C. The solution pH was adjusted by adding small amounts of HNO_3 or KOH, to an appropriate value determined by preliminary experiments. At this pH, no special precautions need be taken to exclude carbon dioxide, because of its extremely low solubility. pH measurements were done by a glass/saturated calomel electrode (Metrohm) standardized before and after each series of pH measurements by NBS standard buffer solutions. A quantity of the support corresponding to a total surface area of about 5 m^2 was suspended in the solution and the suspension was allowed to equilibrate for 20 h, with stirring. Following equilibration, the pH of the suspension was measured and the suspension was filtered through membrane filters (Millipore, 0.22 μm). The filtrate was analyzed spectrophotometrically (Varian Cary 219 UV/VIS) for total molybdenum, Mo_t, at 490 nm (*20*). In each series of adsorption experiments, a blank was included, to make sure that no molybdenum species were adsorbed on the membrane filters or on the walls of the vials used for the adsorption experiments.

The surface concentration of the Mo^{VI}, Γ [mol/m^2], was determined by use of

$$\Gamma = \{v(C_0 - C_{eq})\}/ws, \qquad (1)$$

where C_0, C_{eq}, v, w, and s are the Mo_t concentration before and after adsorption (mol/dm^3), the suspension volume (dm^3), the weight (g), and the specific surface area (m^2/g) of the support, respectively.

It should be noted that preliminary experiments showed that adsorption reached

equilibrium after 2–3 h. Past this time period, the amount of the Mo^{VI} species adsorbed remained constant.

Electronic Spectra of the Molybdate Solutions

The UV spectra of the molybdate solutions were recorded in the range between 370 and 180 nm with a Varian Cary 219 UV/VIS spectrophotometer.

Potentiometric Titrations

In order to study the influence of the adsorption of the molybdates on the surface charge of the support, potentiometric titrations were done on γ-alumina suspensions in the presence of NH_4NO_3. Experiments were done at three different ionic strengths (0.1, 0.06, and 0.01 mol/dm^3, NH_4NO_3 used as background electrolyte) and at constant temperature (25.0 ± 0.1° C). The aqueous suspensions were equilibrated for 20 h before titration. This period was sufficient for a constant value of the suspension pH to be reached. The pH was recorded every 2 min as a function of the volume of titrant added to the suspension. Details concerning the setup and procedure used as well as of the method followed for the determination of the surface charge on each pH have been reported elsewhere (*18, 19*).

Microelectrophoretic Mobility Measurements

The electrophoretic mobility of the support particles was measured with a Rank Brothers particle microelectrophoresis apparatus, Model MKII, by use of a four-electrode thin-walled cylindrical cell, at 25°C. Sufficiently dilute suspensions of γ-alumina particles were prepared in a solution of the background electrolyte both in the absence and in the presence of molybdate ions. In all cases, the experiments were performed at constant ionic strength, 0.01 mol/dm^3, adjusted with NH_4NO_3. The pH of the suspensions was adjusted by small additions of 1 mol/dm^3 HNO_3 or KOH solutions. The velocity of the particles was measured at two depths of the cell where solvent is calculated to be at rest (*21*). Twenty particles were timed over a 30-μm distance for each direction of the electric field to determine an average velocity. From the electrophoretic mobility, defined as the experimental velocity divided by the strength of the electric field, the electrokinetic charge density, σ_{ek}, which is the charge at the shear plane, can be easily calculated at each pH (*22*).

RESULTS

In order to examine whether the positive ($\overline{Al}OH_2^+$) or neutral ($\overline{Al}OH$) surface hydroxyls are the groups mainly responsible for the creation of the sites on which the molybdates are adsorbed, we have selected (*16, 17*) concentration values for the $\overline{Al}OH_2^+$ and $\overline{Al}OH$ as well as values of surface Mo^{VI} concentration corresponding to the monolayer coverage, Γ_m. These values are compiled in Table 1. It is clear that Γ_m increases as the concentration of the $\overline{Al}OH_2^+$ increases while $\overline{Al}OH$ concentration decreases at the same time.

Figure 1 illustrates the variation in the pH measured before, pH_{in}, and after, pH_f, adsorption with C_0. An increase in pH_{in} with C_0 is observed. In all cases adsorption causes an increase in the pH but the difference $pH_f - pH_{in}$, being always positive, decreased as the concentration increased. These phenomena are in agreement with the literature (*1, 5, 23*).

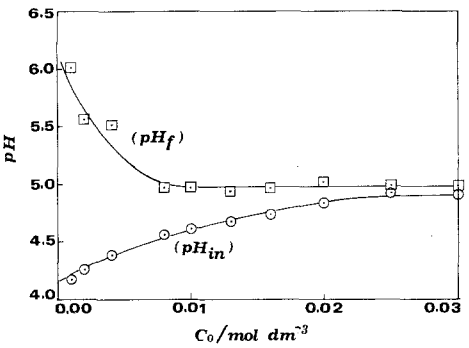

FIG. 1. Illustrates the variation in the pH measured before, pH_{in}, and after, pH_f, adsorption with C_0.

TABLE 1

Concentrations of the $\overline{Al}OH_2^+$ and $\overline{Al}OH$ Groups as well as the Surface Concentrations of the Mo^{VI} Ions, Γ_m, Corresponding to the Monolayer Coverage Determined for Undoped [Nos. 1, 2, and 3] and Na-Doped [No. 4] γ-Alumina under Various Conditions

No.	Support	Conditions pH, T(°C)	Conc. of the $\overline{Al}OH_2^+$ (sites/nm²)	Conc. of the $\overline{Al}OH$ groups[a] (sites/nm²)	Γ_m[b] (atom Mo/nm²)
1	γ-Al_2O_3	5 25	0.3085	7.6189	3.8 ± 0.1
2	γ-Al_2O_3	4 25	1.0372	6.9223	7.5 ± 0.1
3	γ-Al_2O_3	5 55	1.9756	6.0289	8.5 ± 0.2
4	γ-Al_2O_3/Na[c]	5 25	7.1172	0.8828	12.3 ± 0.2

[a] From Refs. (*17*) and (*19*).

[b] Calculated from Eq. (21) (see Discussion). The Γ_m values corresponding to Nos. 2, 3, and 4 have been taken from the second paper of this series.

[c] Contain 0.984 mmol Na^+/g γ-Al_2O_3.

Figure 2 shows the electronic spectra of two (one dilute and one concentrated) molybdate solutions used in the adsorption experiments. In addition, the figure shows the spectrum of a molybdate solution where the MoO_4^{2-} ions are expected to be present almost exclusively (pH 12, $C_0 = 2 \times 10^{-3}$ mol/dm³), and the spectrum of another solution where the isopolyanions are expected to be the dominant species (PH 4, $C_0 = 2 \times 10^{-2}$ mol/dm³). As the concentration of the molybdate solution increased, inside the concentration range used in the adsorption experiments, an increase in the absorption from 0 to 1.40 was progressively extended from 245 nm to higher wavelengths (compare for example curve b with curve c).

Figure 3 illustrates the adsorption isotherm obtained for the adsorption of the molybdates at pH 5, $T = 25$°C, and $I = 0.1$ mol/dm³ NH_4NO_3. The experimental points were fitted well with an *S*-type isotherm. This type of isotherm described also a large number of absorption experiments performed at various pH, temperatures, and doped supports based on γ-alumina.

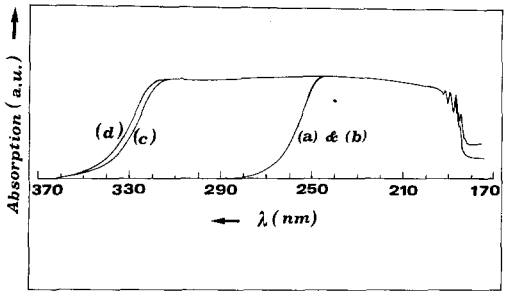

FIG. 2. Electronic spectra of two molybdate solutions used in the adsorption experiments (b, c) and of two molybdate solutions where the MoO_4^{2-} (a) and isopolyanions (d) are the predominant species. (a) pH 12, $C_0 = 2 \times 10^{-3}$ mol/dm³; (b) pH 5.05, $C_0 = 2 \times 10^{-3}$ mol/dm³; (c) pH 5, $C_0 = 2 \times 10^{-2}$ mol/dm³; (d) pH 4, $C_0 = 2 \times 10^{-2}$ mol/dm³.

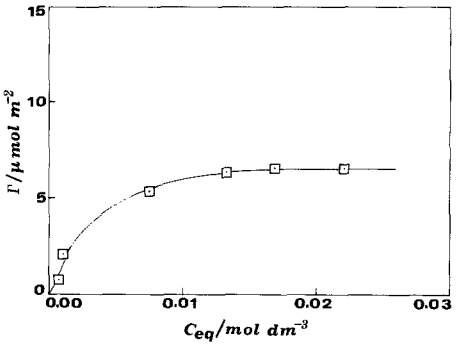

FIG. 3. Variation in the surface concentration of the Mo^{VI}, Γ, with the Mo^{IV} concentration in solution after adsorption of γ-alumina. pH 5, $T = 25$°C, $I = 0.1$ mol/dm³ NH_4NO_3.

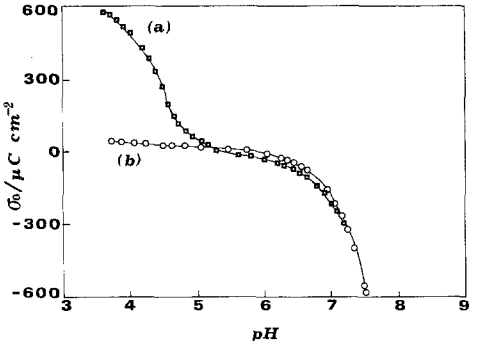

FIG. 4. Surface charge of γ-alumina as a function of pH of suspension at 25°C. (a) Ammonium heptamolybdate solution, $C_0 = 1 \times 10^{-3}$ mol Mo^{VI}/dm^3, $I = 0.1$ mol/dm^3 NH_4NO_3; (b) 0.1 mol/dm^3 NH_4NO_3 solution.

It was found that the presence of molybdates increased the surface charge and decreased the electrokinetic charge density at relatively low pH values. Figures 4 and 5 show typical variations in the surface charge, σ_0, and the electrokinetic charge density, σ_{ek}, achieved in the presence (curves a) and absence (curves b) of the $Mo_xO_y^{z-}$ ions, respectively.

DISCUSSION

On the Nature of the Adsorption Sites

The results compiled in Table 1 strongly suggest that the groups responsible for the creation of the adsorption sites on which the molybdates are located are mainly the protonated surface hydroxyls. This conclusion is corroborated by a significant body of additional results, to be presented in the second paper of this series, dealing with the correlation of the protonated and neutral surface hydroxyls with the adsorption capacity and the γ-alumina determined under various conditions (pH, temperature, dopant concentration). Concerning the "stoichiometry" of the Mo^{VI} deposition, the higher values shown in the fifth column, in comparison with those appearing in the third column, may be attributed to the following:

(i) Participation of the neutral hydroxyls in the adsorption cannot be precluded. It should be noted at this point that this participation in the adsorption process is not necessarily correlated with the undissociated hydroxyl group concentration; i.e., the number of the uncharged groups may be large and yet their interaction minor.

(ii) The concentration of the $\overline{AlOH_2^+}$ groups was determined in the absence of molybdates, a procedure which yields lower concentrations, compared to the results obtained in their presence.

(iii) A contribution to the adsorption of the $Mo_xO_y^{z-}$ ions with $x > 1$ should not be precluded.

Influence of Adsorption and C_0 on pH-Selective Adsorption of MoO_4^{2-}

The main goal of this paragraph is to demonstrate that our view for adsorption via positive sites created mainly by protonated surface hydroxyls is not in conflict with the variation in the pH of the impregnating solution with C_0 as shown in Fig. 1.

As reported by Van Veen *et al.* (5), in addition to the well-known equilibrium

$$Mo_7O_{24}^{6-} + 4H_2O \rightleftarrows 7MoO_4^{2-} + 8H_{aq}^+, \quad (2)$$

another equilibrium may be also involved:

$$Mo_7O_{24}^{6-} + MoO_4^{2-} + 2H_{aq}^+ \rightleftarrows [H_2Mo_8O_{28}]^{6-}. \quad (3)$$

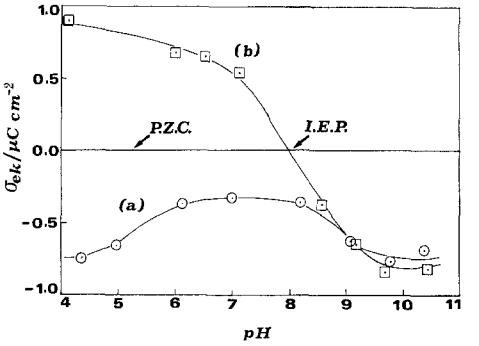

FIG. 5. Electrokinetic charge density of γ-alumina as a function of pH of the suspension at 25°C. (a) Ammonium heptamolybdate solution, $C_0 = 1 \times 10^{-3}$ mol Mo^{VI}/dm^3, $I = 0.01$ mol/dm^3 NH_4NO_3; (b) 0.01 mol/dm^3 NH_4NO_3 solution.

The first equilibrium would have resulted in a decrease and the second in an increase in the dependence of pH_{in} on C_0. Considering therefore the competitive action of (2) and (3) and adopting suitable values for the equilibrium constants, the slight increase in the pH_{in} with the C_0 (Fig. 1) may be explained.

The considerable increase in pH, observed after impregnating the support with relatively dilute molybdate solutions, can be attributed to the protonation of the neutral and deprotonated hydroxyls of γ-alumina (*16–19*).

$$\overline{Al}OH + H_s^+ \rightleftarrows \overline{Al}OH_2^+ \quad (4)$$

$$\overline{Al}O^- + H_s^+ \rightleftarrows \overline{Al}OH \quad (5)$$

$$H_s^+ \rightleftarrows H_{aq}^+ \quad (6)$$

$$H_2O \rightleftarrows H_{aq}^+ + OH_{aq}^-. \quad (7)$$

The protonation equilibria illustrated above were anticipated since the pH values of the molybdate solutions, in the range of the Mo^{VI} concentrations studied, were lower than the point of zero charge of the support (PZC = 5.3). The suggestion that the increase in pH is due to the above-mentioned equilibria and not to the adsorption of the molybdates is corroborated by the observation that γ-alumina causes a similar increase in the pH of KNO_3 and NH_4NO_3 in the absence of molybdate ions. In fact, we have observed that γ-alumina increased the pH of the 0.1 mol/dm^3 KNO_3 and 0.1 mol/dm^3 NH_4NO_3 from 5.28 to 7.49 and from 5.3 to 6.79, respectively, under conditions similar to those followed in the present work.

The decrease in the difference $pH_f - pH_{in}$ with C_0 could be explained assuming that the adsorption constant for the MoO_4^{2-} is larger compared to that for the $Mo_7O_{24}^{6-}$ or $[H_2Mo_8O_{28}]^{6-}$. In that case, the increase in the pH due to the equilibria (4)–(7) may be compensated by the H_{aq}^+ produced due to the displacement of the equilibrium (2) to the right. Obviously the amount of the H_{aq}^+ produced increases with the concentration of the molybdate solution. As mentioned in the Introduction, the assumption concerning the selective adsorption of the MoO_4^{2-} has been supported by experimental evidence (*8, 10–13*).

The progressive decrease in the pH difference mentioned above, with C_0, could be taken as an indication that the contribution of the precipitation to the whole deposition is rather negligible (*5*). However, this point will be investigated more in the third part of this work where a detailed characterization is performed on the specimens studied in the first and second paper of the series.

The above considerations show that it is not necessary to assume that the molybdates react with the neutral hydroxyls (*3, 5–8*) in order to explain the pH variation associated with the adsorption process.

Mo^{VI} Species Present in the Molybdate Solution

The theoretical analysis of the isotherm, described in the last paragraph under Discussion, requires knowledge of whether one or more kinds of $Mo_xO_y^{z-}$ are present in the molybdate solutions used in measuring the isotherm. Such information may be obtained from the electronic spectra. Thus, the spectrum in Fig. 2a, in agreement with the literature (e.g., Ref. (*8*)), shows that the MoO_4^{2-} species absorb in the range 230–245 nm. On the other hand the spectrum in Fig. 2d indicates that the presence of isopolyanions gives rise to an additional broad and structureless band extended from 245 to 320 nm. Although absorption at wavelengths higher than 245 nm, presumably consisting of more than one mutually overlaping bands, can hardly be ascribed to well-defined species, but it is indicative rather, of the presence of the isopolyanions in the ammonium heptamolybdate (AHM) solutions.

It has often been reported in the literature that the predominant Mo^{VI} species depend on the pH of the molybdate solution (e.g., Ref. (*1*): At relatively high and low pH values the MoO_4^{2-} and the various isopolyanions (mainly $Mo_7O_{24}^{6-}$) predomi-

nate. On the other hand it is plausible to expect that the predominant species depend on the concentration of the molybdate solution as well. Comparison of spectrum 2a with spectrum 2b showed that MoO_4^{2-} was predominant even at pH 5 in the case where the molybdate solution is dilute (C_0 = 0.002 mol/dm^3). This is not the case in more concentrated solutions, e.g., C_0 = 0.84 mol/dm^3, where the change in pH from 11 to 6 causes considerable increase in the concentration of the $Mo_7O_{24}^{6-}$ (see Fig. 2, Ref. (*8*)).

Our observation that an increase in the concentration at pH 5 gives rise to an increase in the absorption, from 0 to 1.40, progressively extending from 245 nm to higher wavelengths, could be taken as an indication of a progressive increase in the concentration of isopolyanions with the concentration of the molybdate solution.

These results suggest that it is reasonable to analyze the isotherm on the basis of more than one kind of the $Mo_xO_y^{z-}$ ions present in the solution. Moreover, it seems reasonable to assume that the concentration of a given molybdate is proportional to the total concentration and that the proportionality constants are larger for the isopolyanions compared with that for the MoO_4^{2-}.

Location of the Adsorbed $Mo_xO_y^{z-}$ Ions on the Inner Helmholtz Plane—Qualitative Approach (Fig. 6)

The isotherm shown in Fig. 3 is typical of a large number of similar isotherms, all of which have an S-shape. All of these isotherms were described by the same equation, taking into consideration lateral interactions. The S-type of the isotherm obtained strongly suggests localized, Langmuir-type, adsorption of the $Mo_xO_y^{z-}$ ions on the IHP with considerable lateral interactions (*24, 27*). The shift from the L (Langmuir without lateral interactions) to the S-type isotherm becomes more and more clear as the intensity of the lateral interactions increases (*27*).

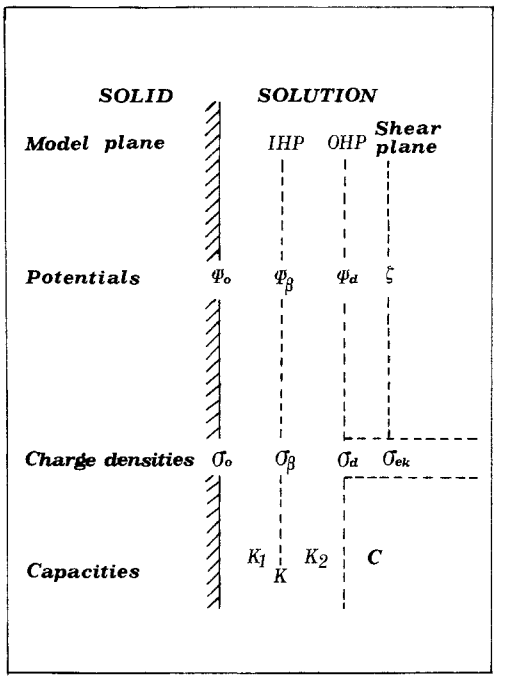

FIG. 6. Structure of the electrical double layer. Triple layer model.

Strong, though qualitative, evidence that the $Mo_xO_y^{z-}$ ions are adsorbed on the IHP was obtained from the study of the influence of adsorption on the σ_0 and σ_{ek} values determined at various pHs (Figs. 4 and 5). In fact, assuming adsorption on the IHP, the influence of the adsorption on the σ_0 values may be explained (Fig. 4): the fact that the adsorption of the negative $Mo_xO_y^{z-}$ ions does not decrease σ_0 demonstrated that these ions are not located on the surface of the support. On the other hand, the observation that the adsorption of the $Mo_xO_y^{z-}$ ions does not change σ_0 considerably at pH greater than the point of zero charge of γ-alumina, where its surface is negatively charged, should be attributed to the relatively low extent of adsorption of the $Mo_xO_y^{z-}$ ions in this pH range. However, the main issue which needs explanation is that adsorption caused an increase in the σ_0 values determined at pH values lower than 5.0 where the surface of the support is positively charged. This increase

was attributed to the formation of additional $\overline{Al}OH_2^+$ groups induced by the $Mo_xO_y^{z-}$ ions located on the IHP. In fact, it should be expected that the presence of the $Mo_xO_y^{z-}$ ions on the IHP may increase and stabilize the surface $\overline{Al}OH_2^+$ groups, presumably by forming ion pairs such as $\overline{Al}OH_2^+ \ldots Mo_xO_y^{z-}$ (*19*). As pH decreased, the extent of adsorption increased as did σ_0.

In order to explain the variation in σ_{ek} with pH in the absence and presence of the $Mo_xO_y^{z-}$ ions (Fig. 5) it should be kept in mind that the σ_{ek} values, determined by microelectrophoretic mobility measurements, refer to the total charge from the surface to the shear plane of the electrical double layer around γ-Al_2O_3 particles (Fig. 6). It is convenient to divide the pH range into the following regions: (i) PZC < pH < IEP, (ii) pH < PZC, and (iii) pH > IEP. First, we deal with the plot of σ_{ek} vs pH, obtained in the absence of the $Mo_xO_y^{z-}$ ions (Fig. 5b). The corresponding schematic representations in Figs. 7a, 7b, and 7c clarify the explanation proposed. Since in range (i) σ_0 is negative (*16, 17*), the positive value of σ_{ek} observed could be explained assuming a small extent of adsorption of the NH_4^+ ions at the IHP. In fact, this adsorption could have produced positive charge near the IHP where the NH_4^+ ions are assumed to be located (Fig. 7a). In range (ii) σ_0 is positive (*16, 17*) and the adsorption of the NH_4^+ ions simply causes an increase in the positive charge (Fig. 7b). In range (iii) the small extent of adsorption of the NH_4^+ ions at the IHP is not sufficient to compensate the relatively high negative charge which the surface is expected to present in this pH range (Refs. (*16, 17*); Fig. 7c). A progressive decrease (increase) in the charge in ranges (i) and (ii) (range (iii)) from the IHP to the solution is to be expected because the charge

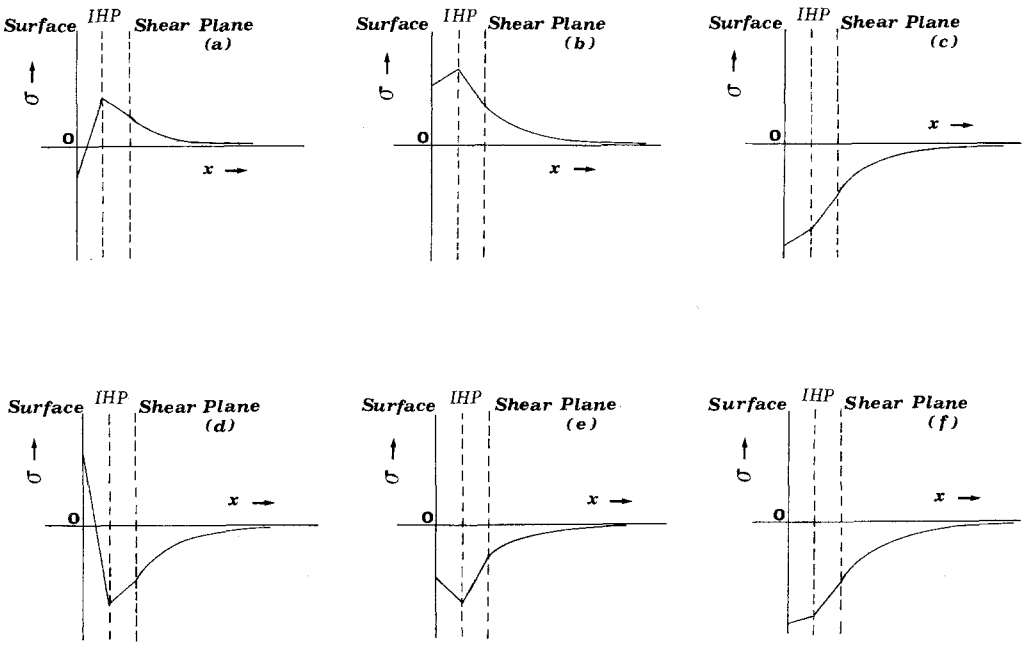

FIG. 7. Schematic representations of the variation in charge with the distance from the surface: (a) region (i), PZC < pH < IEP; (b) region (ii), pH < PZC; (c) region (iii), pH > IEP (in the absence of molybdates (Fig. 5b)); (d) region (ii), pH < PZC; (e) region (i), PZC < pH < IEP; (f) region (iii), pH > IEP (in the presence of molybdates (Fig. 5a)).

of the latter is taken to be equal to zero. It should be noted that K^+ or NO_3^- ions, which are the counter ions of the base or acid added for the pH adjustment, are known to not adsorb specifically onto γ-Al_2O_3 (pure and doped) (*18, 20*).

Let us now discuss the plot of σ_{ek} vs pH obtained in the presence of the $Mo_xO_y^{z-}$ ions (Fig. 5a). The most important observation is that σ_{ek} is negative at all pH values in the pH range 4–11. This observation corroborates the assumption that the $Mo_xO_y^{z-}$ ions are adsorbed on IHP. In fact, the presence of the $Mo_xO_y^{z-}$ ions on the IHP provides an explanation for the negative σ_{ek} observed even at pH < PZC (range ii), where $\sigma_0 > 0$ (Fig. 7d). It should be stressed that in this range as well as in range (i) (Fig. 7e), the adsorption of the $Mo_xO_y^{z-}$ ions should be the dominant process because it compensates for the positive surface charge (range ii) and for the positive charge due to the presence of the NH_4^+ ions (ranges (i) and (ii)). On the other hand in range (iii) (pH > IEP), where the surface has a relatively high negative charge, the extent of adsorption of the $Mo_xO_y^{z-}$ ions becomes relatively low, comparable with the extent of adsorption of the NH_4^+ ions. This explains the observation that in this range the presence of the $Mo_xO_y^{z-}$ ions cannot bring about a large shift in the σ_{ek} to negative values (compare curves a and b of Fig. 5 in the pH range 8–11). Presumably in this range the specifically adsorbed $Mo_xO_y^{z-}$ ions simply compensate for the effect of the adsorbed NH_4^+ ions (Fig. 7f). The quite complicated form of Fig. 5a should be attributed to the fact that the pH change alters both the surface charge, and consequently the extent of the specific adsorption, and the relative concentration of the various molybdates present in the solution. It is important to note that Fig. 5a obtained in the presence of the $Mo_xO_y^{z-}$ ions precluded the assumption that these ions are located at the diffuse part of the double layer. In fact, this is obvious concerning range (iii) where the charge up to the IHP is negative, requiring positive counter ions. With respect to ranges (i) and (ii) it might be argued that since the charge up to the IHP is positive (Figs. 7a and 7b) the negative $Mo_xO_y^{z-}$ ions could be located in the diffuse part of the double layer as counter ions. But in that case a positive charge should be expected until the shear plane (Figs. 7a and 7b) in disagreement with the negative charge determined experimentally (Figs. 5a, 7e, and 7d).

In conclusion a first examination of the isotherm as well as the study of the effect of the $Mo_xO_y^{z-}$ ion adsorption on the σ_0 and σ_{ek} determined at various pHs strongly suggests that the adsorbed $Mo_xO_y^{z-}$ are located on the IHP, whereas lateral interactions are exerted between the adsorbed $Mo_xO_y^{z-}$ ions. It can also be concluded that the adsorption of $Mo_xO_y^{z-}$ ions on the IHP predominates in the range 4 < pH < IEP, whereas at pH > IEP it becomes comparable with the adsorption of the NH_4^+ ions.

Location of the Adsorbed $Mo_xO_y^{z-}$ Ions on the Inner Helmholtz Plane—Quantitative Approach

From the considerations presented in the previous paragraph it seems reasonable to attempt an analysis of the isotherm based on the assumption that the $Mo_xO_y^{z-}$ ions are located on the IHP. In particular it seems interesting to examine whether our experimental results could be described by a Stern–Laungmuir equation, now derived on the assumption that more than one kind of the $Mo_xO_y^{z-}$ ions are present in the solution, which implies adsorption at the IHP without lateral interactions (*24*) or by a Stern–Langmuir–Fowler isotherm which takes into account lateral interactions (*25*).

Specifically Adsorbed $Mo_xO_y^{z-}$ Ions on the IHP—No Considerable Lateral Interactions

First we assume that all kinds of $Mo_xO_y^{z-}$ ions could be adsorbed on the IHP and that no lateral interactions are exerted between them. Next, we focus on the ith kind of the

$Mo_xO_y^{z-}$ ions. Assuming that one specifically adsorbed ion, i, replaces one water molecule, 1, from the IHP we may write for the equilibrium

$$i^L + 1^I \rightleftarrows i^I + 1^L, \quad (8)$$

where L and I stand, respectively, for the bulk solution and IHP. The following equations provide the electrochemical potentials of the entities involved in the above equilibrium (*25*):

$$\begin{aligned}
\tilde{\mu}_i^L &= \mu_i^{0,L} + RT \ln x_i + Z_i F \Phi_L \\
\tilde{\mu}_i^I &= \mu_i^{0,I} + RT \ln \theta_i + Z_i F \Phi_A \\
&\quad + g_i(\Phi'_A, \Phi''_A, \ldots) \quad (9) \\
\tilde{\mu}_1^I &= \mu_1^{0,I} + RT \ln[1 - \Sigma_i \theta_i] \\
&\quad + g_1(\Phi'_A, \Phi''_A, \ldots) \\
&= \mu_1^{0,I} + RT \ln[1 - \theta] \\
&\quad + g_1(\Phi'_A, \Phi''_A, \ldots) \\
\tilde{\mu}_1^L &= \mu_1^{0,L} + RT \ln[1 - \Sigma_i x_i],
\end{aligned}$$

where $\tilde{\mu}_1$, $\tilde{\mu}_i$, μ_1^0, μ_i^0, x_i, Z_i, θ_i, θ, $g_1(\Phi'_A, \Phi''_A, \ldots)$ and $g_i(\Phi'_A, \Phi''_A, \ldots)$ represent the electrochemical potential for the water and i, the corresponding standard state chemical potentials, the molar ratio and the charge of i, the fraction of the sites covered by i and all kinds of $Mo_xO_y^{z-}$ ions and functions of derivatives of Φ_A for the water and i. Φ_L and Φ_A represent, respectively, the Galvani potential in the liquid phase and in the adsorption site A. The first and second derivatives of the Galvani potential involved in these functions are related, respectively, to the dipolar and tetrapolar moments of the water molecules at the interface (*25*). According to equilibrium (8),

$$\tilde{\mu}_i^L + \tilde{\mu}_1^I = \tilde{\mu}_i^I + \tilde{\mu}_1^L. \quad (10)$$

Replacing the electrochemical potentials involved in the above equation by the corresponding right-hand sides of Eqs. (9) we have

$$\begin{aligned}
\theta_i/(1 - \theta) &= x_i/(1 - \\
&\Sigma_i x_i) \exp\{[(-\Delta G^\circ_{\text{Chem},i}) + (-\Delta G^\circ_{\text{elect},i}) \\
&\quad + (-\Delta G^\circ_{\text{dip,tetrap}})]/RT\}, \quad (11)
\end{aligned}$$

where

$$-\Delta G^\circ_{\text{Chem},i} = [\mu_i^{0,L} + \mu_1^{0,I}] - [\mu_i^{0,I} + \mu_1^{0,L}],$$

$$-\Delta G^\circ_{\text{elect},i} = Z_i F(\Phi_L - \Phi_A) = -Z_i F \Psi_{IHP}$$

and

$$-\Delta G^\circ_{\text{dip,tetrap}} = g(\Phi'_A, \Phi''_A, \ldots)$$

represent the contribution to the standard free energy of adsorption $\Delta G^\circ_{\text{ads},i}$ of the chemical, electrostatic, and dipolar–tetrapolar interactions. Ψ_{IHP}, assumed equal to $\Phi_A - \Phi_L$ (*26*), represents the potential at IHP. From Eq. (11) one can easily obtain the Stern–Langmuir equation for ion i,

$$\begin{aligned}
\theta_i/(1 - \theta) &= C_{\text{eq},i}/55.5 \exp[-\Delta G^\circ_{\text{ads},i}/RT] \\
&= C_{\text{eq},i} K_i, \quad (12)
\end{aligned}$$

where

$$\Delta G^\circ_{\text{ads},i} = \Delta G^\circ_{\text{Chem},i} + \Delta G^\circ_{\text{elect},i} + \Delta G^\circ_{\text{dip,tetrap}}$$

and

$$K_i = (1/55.5) \exp[-\Delta G^\circ_{\text{ads},i}/RT].$$

$C_{\text{eq},i}$ represents the equilibrium concentration of the ions i.

It should be noted that usually $\Delta G^\circ_{\text{dip,tetrap}}$ is negligible compared to the $\Delta G^\circ_{\text{Chem},i}$ and $\Delta G^\circ_{\text{elect},i}$. Equation (12) is valid for each kind of $Mo_xO_y^{z-}$ ion. Therefore, for all kinds of $Mo_xO_y^{z-}$ ions we have

$$\begin{aligned}
&\Sigma_i[\theta_i/(1 - \theta)] = \theta/(1 - \theta) \\
&= \Sigma_i[(C_{\text{eq},i}/55.5) \exp(-\Delta G^\circ_{\text{ads},i}/RT)]. \quad (13)
\end{aligned}$$

In agreement with the results from the electronic spectra, we assume that $C_{\text{eq},i}$ is proportional to the total equilibrium concentration, C_{eq}, which is determined experimentally:

$$C_{\text{eq},i} = a_i C_{\text{eq}}. \quad (14)$$

Apparently, coefficient a_i, being independent of C_{eq}, is a function of the temperature, pH, and the nature of the species i. Combining Eq. (13) with Eq. (14) we obtain

$$\begin{aligned}
&\theta/(1 - \theta) \\
&= C_{\text{eq}} \Sigma_i[(a_i/55.5) \exp(-\Delta G^\circ_{\text{ads},i}/RT)], \\
&\quad (15)
\end{aligned}$$

which is reduced to

$$\theta/(1 - \theta) = C_{eq}K, \qquad (16)$$

where $K = \Sigma_i[(a_i/55.5)\exp(-\Delta G^\circ_{ads,i}/RT)]$. Replacing θ with Γ/Γ_m, where Γ is the surface concentration of Mo^{VI} for all kinds of the $Mo_xO_y^{z-}$ ions determined experimentally using Eq. (1) and Γ_m is the corresponding monolayer concentration, Eq. (16) becomes

$$1/\Gamma = 1/K\Gamma_m C_{eq} + 1/\Gamma_m. \qquad (17)$$

An analogous equation may be easily obtained for the i ions by replacing θ_i with Γ_i/Γ_m and θ with Γ/Γ_m in Eq. (12),

$$1/\Gamma_i = 1/K_i\Gamma_{m,i}C_{eq,i} + 1/\Gamma_{m,i}, \qquad (18)$$

where Γ_i and $\Gamma_{m,i}$ represent the surface concentration with respect to the ions i and the corresponding monolayer concentration. Equation (18) can be tested for the cases in which only the i ions are present or when we may selectively determine the concentration of this kind of $Mo_xO_y^{z-}$ ion. In contrast, Eq. (17) may be tested in our case. It predicts a straight line for the plot $1/\Gamma$ vs $1/C_{eq}$, provided that all kinds of the adsorbed $Mo_xO_y^{z-}$ ions are located on distinct, energetically equivalent, sites of the IHP, where no lateral interactions are exerted between these ions. Figure 8 shows that this is not the case and this suggests that at least one of the assumptions mentioned is not valid. It should be mentioned that this failure in matching the isotherms using Eq. (17) is pronounced in all cases examined in the second paper of this series (isotherms obtained at different pHs, temperatures, and dopant concentrations).

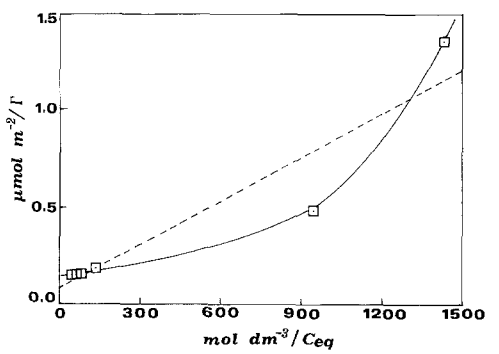

FIG. 8. Reciprocal surface concentration of Mo^{VI} as a function of $1/C_{eq}$. The dashed line represents the values calculated using Eq. (17).

Specifically Adsorbed $Mo_xO_y^{z-}$ Ions on the IHP—Considerable Lateral Interactions

In the following we keep the assumptions made in the previous paragraph but now we assume that marked interactions exist between the adsorbed $Mo_xO_y^{z-}$ ions. Moreover, we assume that the magnitude of these interactions is practically independent of the kind of $Mo_xO_y^{z-}$ ions. Taking into account that in most cases $\Delta G^\circ_{dip,tetrap}$ is negligible compared with $\Delta G^\circ_{chem,i}$ and $\Delta G^\circ_{elect,i}$, we may write

$$\Delta G^\circ_{ads,i} = \Delta G^\circ_{chem,i} + \Delta G^\circ_{elect,i}.$$

Moreover, following Hough and Rendall (*28*) we consider that

$$\Delta G^\circ_{chem,i} = \Delta G^\circ_{cs,i} + \Delta G^\circ_{cc},$$

where $\Delta G^\circ_{cs,i}$ and ΔG°_{cc} represent the contribution to the $\Delta G^\circ_{chem,i}$ of the chemical interactions between $Mo_xO_y^{z-}$ ions and support and of the chemical interactions between the adsorbed $Mo_xO_y^{z-}$ ions. Finally, we assume that $\Delta G^\circ_{cc} = -E\theta$, where E is the energy of lateral interactions (*29*). From the above one may obtain

$$\Delta G^\circ_{ads,i} = Z_iF\Psi_{IHP} + \Delta G^\circ_{cs,i} - E\theta$$
$$= Z_iF\Psi_{IHP} + \Delta G^\circ_{cs,i} - \lambda\Gamma, \qquad (19)$$

where λ is a constant equal to E/Γ_m. Combination of Eq. (19) with Eq. (15) provides

$$\theta/(1 - \theta) = \tilde{K}C_{eq}\exp[\lambda\Gamma/RT], \qquad (20)$$

where the constant $\tilde{K}$ is equal to

$$\Sigma_i[(a_i/55.5)\exp(-Z_iF\Psi_{IHP}/RT - \Delta G^\circ_{cs,i}/RT)].$$

From Eq. (20) the following relationship may be obtained, which is similar to the equation of de Keiser and Lyklema (*25*),

$$1/\Gamma = 1/\Gamma_m + 1/\Gamma_m\tilde{K}C_{eq}\exp[\lambda\Gamma/RT]. \qquad (21)$$

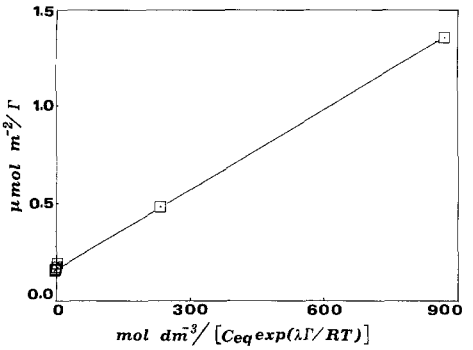

FIG. 9. Reciprocal surface concentration of Mo^{VI} as a function of $(1/C_{eq})\exp(\lambda\Gamma/RT)$. The solid line represents the values calculated using Eq. (21).

An analogous equation can be easily derived for the ions i:

$$1/\Gamma_i = 1/\Gamma_{m,i} + 1/\Gamma_{m,i}\tilde{K}_i C_{eq,i} \exp(\lambda\Gamma/RT). \quad (22)$$

In Eq. (22), the constant $\tilde{K}_i$ is equal to

$$(1/55.5)\exp[-Z_i F\Psi_{IHP}/RT - \Delta G^\circ_{cs,i}/RT].$$

Equation (22) can be tested only in the cases mentioned for Eq. (18). On the contrary Eq. (21) can be tested in our case. Figure 9 shows that the plot $1/\Gamma$ vs $(1/C_{eq})\exp(\lambda\Gamma/RT)$ describes our experimental data very well. The above confirm that the adsorbed $Mo_xO_y^{z-}$ ions are located on energetically equivalent distinct sites of the IHP of the double layer and that considerable lateral interactions are exerted between these species.

It should be noted that Eq. (21) is valid even in the case where only one kind, for instance j, of $Mo_xO_y^{z-}$ is adsorbed. In that case $\tilde{K}$ is equal to

$$(a_j/55.5)\exp[-Z_j F\Psi_{IHP}/RT - \Delta G^\circ_{cs,j}/RT].$$

Therefore, the analysis of the isotherm cannot help us solve the dilemma of whether

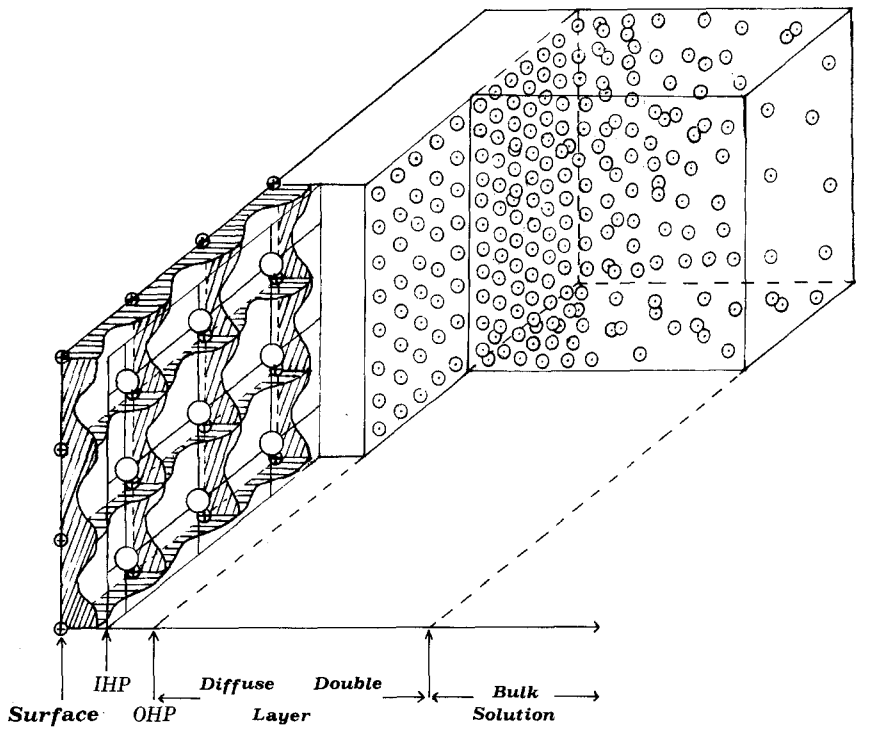

FIG. 10. The mechanism of adsorption of the $Mo_xO_y^{z-}$ ions on γ-Al_2O_3: (⊕) Protonated surface hydroxyl, (○) $Mo_xO_y^{z-}$ ion, (⊙) counter ion. Water molecules and other ions are omitted. Shaded regions represent the variation in the potential near the surface (Ref. (*24*)).

only MoO_4^{2-} or more kinds of $Mo_xO_y^{z-}$ ions are adsorbed on the γ-alumina surface.

CONCLUSIONS

From the present work the following conclusions may be drawn: (i) Deposition of Mo^{VI} on the γ-alumina surface takes place via adsorption; the contribution of the precipitation is negligible under our experimental conditions [C_0: $(10^{-3} - 3 \times 10^{-2})$mol Mo^{VI}/dm^3, pH 5, $T = 25°C$, filtration]. (ii) Specifically, the deposition of the Mo^{VI} occurred by adsorption of the $Mo_xO_y^{z-}$ ions on energetically equivalent and distinct sites of the inner Helmholt plane of the double layer that develops between the surface of the γ-Al_2O_3 particles and the solution. The creation of these sites was attributed mainly to the presence of the protonated surface hydroxyls of γ-alumina and not to the neutral hydroxyls. (iii) Considerable lateral interactions are exerted between the adsorbed $Mo_xO_y^{z-}$ ions. (iv) The analysis of the isotherm did not allow determination of whether polymolybdates are first dissociated into MoO_4^{2-} before adsorbing or whether they are adsorbed intact, although to explain the influence of adsorption and Mo^{VI} concentration on the pH of the molybdate solutions it was necessary to assume that the adsorption constant for the MoO_4^{2-} should be larger than those of the polymolybdates.

Figure 10 depicts the mechanism of adsorption of the $Mo_xO_y^{z-}$ ions on γ-alumina which takes into account these conclusions. We believe that in the drying step, in which the elimination of water molecules results in the disappearance of the double layer, the series $Mo_xO_y^{z-}$ . . . $Mo_xO_y^{z-}$ . . . is deposited on the surface from the IHP.

ACKNOWLEDGMENTS

Partial financial support for this project from the Greek Award Granting Authority (IKY) is gratefully acknowledged. We also express our thanks to Mrs. A. Didachou for the preparation of the manuscript.

REFERENCES

1. Wang, L., and Hall, W. K., *J. Catal.* **77,** 232 (1982).
2. Kasztelan, S., Grimblot, J., Bonnelle, J. P., Payen, E., Toulhoat, H., and Jacquin, Y., *Appl. Catal.* **7,** 91 (1983).
3. Iannibello, A., Marengo, S., Trifiro, F., and Villa, P. L., *in* "2nd Int. Sym. on Scientific Basis for the Preparation of Heterogeneous Catalysts, Louvain La Neuve, Belgium, 1978," paper A5.
4. Caceres, C. V., Fierro, L. G., Agudo, A. L., Blanco, M. N., and Thomas, H. J., *J. Catal.* **95,** 501 (1985).
5. Van Veen, J. A. R., De Wit, H., Emeis, C. A., and Hendriks, P. A. J. M., *J. Catal.* **107,** 579 (1987).
6. Iannibello, A., and Mitchell, P. C. H., in "2nd Int. Sym. on Scientific Basis for the Preparation of Heterogeneous Catalysts, Louvain La Neuve, Belgium, 1978," paper E2.
7. Van Veen, J. A. R., and Hendriks, P. A. J. M., *Polyhedron* **5,** 75 (1985).
8. Jeziorowski, H., and Knözinger, H., *J. Phys. Chem.* **83,** 1166 (1979).
9. Houalla, M., Kibby, C. L., Petrakis, L., and Hercules, D. M., *J. Catal.* **83,** 50 (1983).
10. Luthra, N. P., and Cheng, W. C., *J. Catal.* **107,** 154 (1987).
11. Knözinger, H., and Jeziorowski, H., *J. Phys. Chem.* **82,** 2002 (1978).
12. Medema, J., van Stam, C., de Beer, V. H. J., Konings, A. J. A., and Koningsberger, D. C., *J. Catal.* **53,** 386 (1978).
13. Sonnemans, J., and Mars, P., *J. Catal.* **31,** 209 (1973).
14. Wang, L., and Hall, W. K., *J. Catal.* **66,** 251 (1980).
15. Wang, L., and Hall, W. K., *J. Catal.* **83,** 242 (1983).
16. Akratopulu, K., Vordonis, L., and Lycourghiotis, A., *J. Chem. Soc. Faraday Trans 1* **82,** 3697 (1986).
17. Vordonis, L., Koutsoukos, P. G., and Lycourgiotis, A., *J. Chem. Soc. Chem. Commun.*, 1309 (1984).
18. Vordonis, L., Koutsoukos, P. G., and Lycourghiotis, A., *J. Catal.* **98,** 296 (1986).
19. Vordonis, L., Koutsoukos, P.G., and Lycourghiotis, A., *J. Catal.* **101,** 186 (1986).
20. Snell, F. D., "Photometric and Fluorometric Methods of Analysis of Metals," Vol. 2, p. 1296. Wiley, NY, 1978.
21. Overbeek, J. Th. G., *in* "Colloid Science" (H. R. Kruyt, Ed.), p. 219. Vol. 1, Elsevier, Amsterdam, 1952.
22. Wiersema, P. H., Loeb, A. L., and Overbeek, J. Th. G., *J. Colloid Interface Sci.* **22,** 78 (1966).
23. Tsigdinos, G. A., Chen, H. Y., and Streusand,

B. J., *Ind. Eng. Chem. Prod. Res. Dev.* **20,** 619 (1981).
24. Lyklema, J., *in* "Adsorption from Solution at the Solid Liquid Interface" (G. D. Parfitt and C. H. Rochester, Eds.), Chapt. 5. Academic Press, London, 1983.
25. de Keizer, A., and Lyklema, J., *J. Colloid Interface Sci.* **75,** 171 (1980).
26. Vordonis, L., "Regulation of the Surface Charge of Catalytic Carriers Using Several Dopants," Chapts. 3 and 4. PhD thesis, University of Patras, Patras, Greece, 1988.
27. Giles, C. H., Smith, D., and Huitson, A., *J. Colloid Interface Sci.* **47,** 755 (1974).
28. Hough, D. B., and Rendall, H. M., *in* "Adsorption from Solution at the Solid/Liquid Interface" (G. D. Parfitt and C. H. Rochester, Eds.), Chapt. 6. Academic Press, London, 1983.
29. Jaycock, M. J., and Parfitt, G. D., "Chemistry of Interfaces." Wiley, NY, 1981.